THE JOURNAL OF PHYSICAL CHEMISTRY B

Article

pubs.acs.org/JPCB

What Is the Preferred Conformation of Phosphatidylserine–Copper(II) Complexes? A Combined Theoretical and Experimental Investigation

Kari Kusler,[†] Samuel O. Odoh,[†,§] Alexey Silakov,[‡] Matthew F. Poyton,[‡] Saranya Pullanchery,[‡] Paul S. Cremer,[*,‡] and Laura Gagliardi[*,†]

[†]Department of Chemistry, Chemical Theory Center, and Minnesota Supercomputing Institute, University of Minnesota, 207 Pleasant Street SE, Minneapolis, Minnesota 55455-0431, United States

[‡]Department of Chemistry, The Pennsylvania State University, 104 Chemistry Building, University Park, Pennsylvania 16802, United States

Supporting Information

ABSTRACT: Phosphatidylserine (PS) has previously been found to bind Cu^{2+} in a ratio of 1 Cu^{2+} ion per 2 PS lipids to form a complex with an apparent dissociation constant that can be as low as picomolar. While the affinity of Cu^{2+} for lipid membranes containing PS lipids has been well characterized, the structural details of the Cu–PS_2 complex have not yet been reported. Coordinating to one amine and one carboxylate moiety on two separate PS lipids, the Cu–PS_2 complex is unique among ion–lipid complexes in its ability to adopt both *cis* and *trans* conformations. Herein, we determine which stereoisomer of the Cu–PS_2 complex is favored in lipid bilayers using density functional theory calculations and electron paramagnetic resonance experiments. It was determined that a conformation in which the nitrogen centers are *cis* to each other is the preferred binding geometry. This is in contrast to the complex formed when two glycine molecules bind to Cu^{2+} in bulk solution, where the *cis* and *trans* isomers exist in equilibrium, indicating that the lipid environment has a significant steric effect on the Cu^{2+} binding conformation. These findings are relevant for understanding lipid oxidation caused by Cu^{2+} binding to lipid membrane surfaces and will help us understand how ion binding to lipid membranes can affect their physical properties.

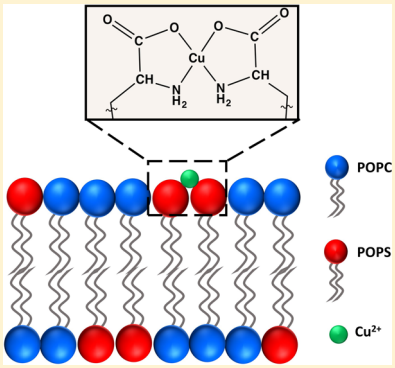

INTRODUCTION

Phosphatidylserine (PS) is the most common negatively charged lipid in mammalian cell membranes.[1] In healthy cells, PS lipids are actively transported to the cytoplasmic leaflet of the cell membrane[2] and play important roles in many physiological processes including apoptosis[2] and blood clotting.[3] PS lipids also function as binding sites for specific proteins and divalent cations.[4−7] Being negatively charged, divalent cations readily bind to PS lipid headgroups.[7] Upon binding, divalent cations can exert dramatic and physiologically relevant changes on the physical properties of lipid membranes. For example, divalent cation binding to PS lipid headgroups can induce domain formation, lipid phase separation,[8−10] and increase the gel to liquid crystalline phase transition temperature of lipid bilayers.[11] Exposure to divalent cations will also cause vesicles containing PS lipids to aggregate or fuse together.[12,13]

The changes in the physical properties of lipid membranes and induction of vesicle fusion and aggregation caused by divalent cation binding to PS lipids are ion-specific. A well-studied example of ion specificity is the ability of Ca^{2+} to induce the fusion of lipid vesicles more readily than Mg^{2+}, an intriguing observation considering that both ions have a similar affinity for PS lipid headgroups.[13,14] The difference in the ability to fuse lipid vesicles together is thought to be caused by Ca^{2+} and Mg^{2+} binding to different locations on the PS lipid headgroup. Molecular dynamics simulations suggest that, while both Ca^{2+} and Mg^{2+} can bind to two separate PS lipid headgroups, Ca^{2+} binds to oxygen atoms on both the phosphate and carboxylate groups, whereas Mg^{2+} binds to either phosphate or carboxylate oxygen atoms on PS lipid headgroups but not both simultaneously.[14] This example illustrates that it is vital to determine exactly how ions bind to specific lipids in order to understand how divalent cation binding can affect the physical properties of lipid membranes.

It has recently been found that Cu^{2+} can bind to PS lipids. Lipid membranes containing transition metal ion–lipid complexes have been referred to as metallomembranes.[15] In stark contrast to divalent cations such as Ca^{2+} and Mg^{2+}, which bind to PS with dissociation constants of 83 and 125 mM, respectively,[7] Cu^{2+} binds to PS with a picomolar dissociation constant.[16,17] This is due to the ability of Cu^{2+} to

Received: October 23, 2016
Revised: November 21, 2016
Published: November 28, 2016

DOI: 10.1021/acs.jpcb.6b10675
J. Phys. Chem. B 2016, 120, 12883−12889

simultaneously coordinate to the carboxylate and amine moieties of two separate PS lipid headgroups.[16] The primary coordination sphere of the Cu−PS_2 complex is identical to that of the bis(glycinato)copper(II) complex formed where Cu^{2+} binds to two glycine molecules in bulk solution.[18] Coordinating to two PS lipid headgroups in this manner introduces the ability to form stereoisomers, a *cis* and a *trans* Cu−PS_2 complex, as shown in Figure 1. To the best of our knowledge, this property

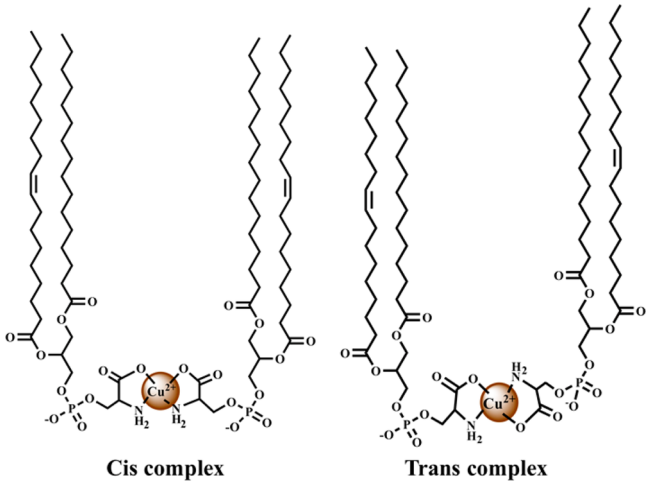

Figure 1. Two possible stereoisomers of the square planar complex formed by Cu^{2+} and PS lipids.

of ion−lipid complexes has not been observed previously. However, in bulk solution, Cu^{2+} can form both *cis*- and *trans*-bis(glycinato)copper(II) complexes.[19] While the *trans* complex is favored thermodynamically,[20] EPR studies have shown that bis(glycinato)copper(II) exists as a mixture of *cis* and *trans* stereoisomers in bulk solution at room temperature.[19,21,22] Therefore, the analogous question in membranes is whether the Cu−PS_2 complex should be *cis* or *trans*.

While the first coordination sphere of the bis(glycinato)-copper(II) complex and the Cu−PS_2 complex are identical, the rest of the ligand environment differs dramatically. Therefore, it is not known if Cu^{2+} prefers to bind to PS lipid headgroups in either a *cis* or *trans* geometry. To elucidate the stereochemistry of the complex between Cu^{2+} and two PS lipids, a combined theoretical and experimental study of this interaction was undertaken. Herein, we use density functional theory (DFT) calculations and electron paramagnetic resonance (EPR) experiments to show that Cu^{2+} prefers to bind to PS lipids in the *cis* configuration. The formation of the *cis* instead of the *trans* complex may have relevance for lipid oxidation, domain formation, or the fusion of lipid vesicles containing PS lipids.

MATERIALS AND METHODS

1-Palmitoyl-2-oleoyl-*sn*-glycero-3-phosphocholine (POPC) and 1-palmitoyl-2-oleoyl-*sn*-glycero-3-phospho-L-serine (POPS) were purchased from Avanti Polar Lipids (Alabaster, AL). Copper(II) chloride ($CuCl_2$, 99.999% trace metal basis) was purchased from Sigma-Aldrich (St. Louis, MO). 3-(4-Morpholinyl) propanesulfonic acid (MOPS, 99%) was purchased from Alfa Aesar (Haverhill, MA). Sodium chloride (NaCl, >99%) was purchased from Dot Scientific (Burton, MI). D_2O (D, 99.9%) was purchased from Cambridge Isotope Laboratories (Tewksbury, MA). While the binding of Cu^{2+} to lipid headgroups could increase the rate of lipid oxidation, we found that oxidation is only increased in the presence of an oxidant that reacts with Cu^{2+} to generate reactive oxygen species, such as hydrogen peroxide. When incubated with Cu^{2+} alone, vesicles containing the Cu^{2+}-binding lipid phosphatidylethanolamine showed no indications of lipid oxidation. We do not expect a large amount of lipids to be oxidized in current experiments either, as there is no chemical that can react with lipid-bound Cu^{2+} to produce reactive oxygen species.

DFT Calculations. The interactions of PS with Cu^{2+} were studied using a model that contained the entire PS headgroup. Both lipid chains after the ester groups in the tails were replaced with hydrogen atoms. Calculations were performed using a cluster of two PS lipids and one Cu^{2+} ion. To mimic the experimental findings about the behavior of PS when interacting with Cu^{2+}, the amino groups were deprotonated, resulting in a net charge of −2 for each PS headgroup. To determine the preferred binding sites of Cu^{2+} to PS, the geometries of a large variety of conformations were optimized with particular focus on the corresponding *cis* and *trans* structures. The free energies were then compared. As Cu^{2+} interactions with PS have been studied very little, the coordination number of this complex is not known. Therefore, the number of water molecules included in the calculations was determined by explicitly adding water molecules coordinated to Cu^{2+} until they no longer stabilized the system or remained within 3 Å of Cu^{2+} after optimization. While this is not a definitive way to determine the coordination number,[23] calculations using varying numbers of water molecules showed the same trend in preferred binding conformations.

After the binding conformation with the lowest energy was determined, the preference for the negatively charged Cu−PS_2 cluster relative to a neutral Cu−PS_2 cluster was examined in order to compare with previous experimental results. This was done by first optimizing the Cu−PS_2 clusters with the amino group not deprotonated, making the clusters electrically neutral. The free energy difference between the negatively charged and the neutral cluster were calculated using eq 1. Two water molecules are present on the left side of the equation because Cu^{2+} was coordinated to two more water molecules in the neutral cluster than in the negatively charged cluster. The previously reported[24] free energy of H^+ corrected for a pH of 8 was used, as it is known that Cu^{2+} will bind to PS at this pH.[16,17]

$$[CuPS_2OH_2]^{2-} + 2H_2O + 2H^+ \rightarrow [CuPS_2(OH_2)_3] \quad (1)$$

A simpler model used to gain additional insight into the binding conformation involved Cu(II)−bis(glycinato) monohydrate. We also considered a model with no explicit water molecules and one with two explicit water molecules bound to the system. Similar trends were observed in all three cases, and we thus report only results from the monohydrate species.

Calculations on the systems described above were performed in Gaussian 09[25] using DFT with the functionals B3LYP-D3,[26−29] M06-L,[30] and M06[31] with triple-ζ polarized basis sets from Ahlrichs and co-workers.[32,33] B3LYP was chosen because it has been used successfully to study similar systems,[20,34−38] and the D3 correction was added to account for long-range dispersion interactions. M06 and M06-L were used because they perform well for systems involving transition metals.[31] The doublet electronic state was considered, and frequencies were calculated in all cases. Starting conformations were chosen manually. When water was involved in the reactions, the total

DOI: 10.1021/acs.jpcb.6b10675
J. Phys. Chem. B 2016, 120, 12883−12889

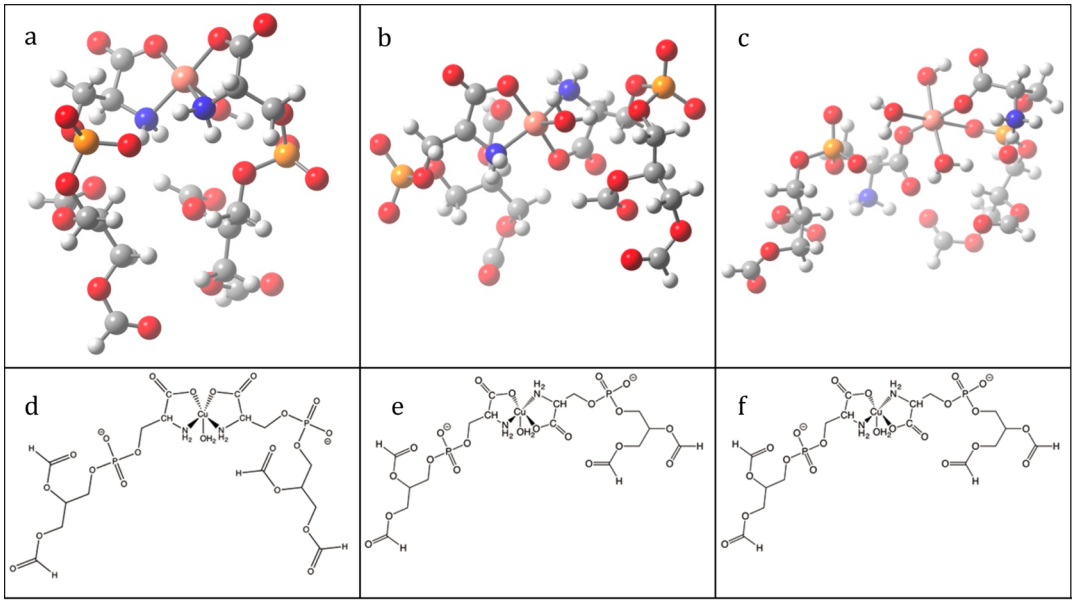

Figure 2. Optimized three-dimensional structures of the *cis* (a), *trans* (b), and neutral (c) configurations of PS bound to Cu^{2+} (carbon is gray, copper is salmon, hydrogen is white, nitrogen is blue, oxygen is red, and phosphorus is orange) and two-dimensional representations, in the same order (d, e, f).

free energy was obtained by adding the experimental free energy of hydration[39] to the calculated gas-phase free energy. Unless otherwise noted, all calculations were performed in solution with water represented with the polarizable continuum model using the integral equation formalism.[40]

For comparison with experiments, EPR *g*-factors and hyperfine coupling constants were determined using the ADF (Amsterdam Density Functional) program.[41] The optimized *cis* and *trans* geometries obtained with the M06 functional were used for these calculations. The spin−orbit zero order regular approximation (ZORA) was used to include relativistic effects,[42,43] and solvent effects of water were included using the conductor-like screening model (COSMO).[44,45] EPR calculations were performed with B3LYP, M06, and M06-L using Slater-type triple-ζ doubly polarized (TZ2P) basis sets.

Vesicle Preparation. Small unilamellar phospholipid vesicles were prepared by freeze−thaw and extrusion techniques.[46,47] POPS and POPC lipids were mixed in a 1:1 ratio in chloroform, and the solvent was evaporated under nitrogen. The dried lipids were placed under a vacuum for 2 h, to remove any residual chloroform. Subsequently, the lipid film was rehydrated in 10 mM MOPS buffer containing 100 mM NaCl and 200 μM $CuCl_2$ in D_2O at pH 7.4. The total concentration of lipids in the buffer solution was 15 mg/mL. Ten freeze−thaw cycles were conducted on the lipid solution using liquid nitrogen and hot water. Then, the lipids were extruded 10 times through a polycarbonate membrane with 400 nm pores (Whatman, Florham Park, NJ). Vesicle size was determined using dynamic light scattering (90 Plus Particle Size Analyzer, Brookhaven Instrument Corp., Holtsville, NY). The average diameter was 287 ± 3 nm.

EPR Experiments. CW EPR measurements were performed using a Bruker ESP 300 X-band spectrometer with an ER 041MR microwave bridge. An ER4116DM cavity operated in the perpendicular TE102 microwave mode was used to collect all spectra. Cryogenic temperatures were achieved using an ER4112-HV Oxford Instruments variable temperature helium flow cryostat.

Data analysis and manipulation were performed using Kazan Viewer.[48] Simulations were performed using homemade programs in MatLabTM utilizing the "pepper" routine from the EasySpin package.[49] The simulated EPR spectrum of vesicles prepared in D_2O accounts for the presence of one anisotropically coupled Cu^{2+} nucleus with the natural abundance of ^{63}Cu(69.17%) and ^{65}Cu (30.83%) isotopes as well as two equivalent ^{14}N nuclei with isotropic HF coupling. To reproduce the overall line shape, an anisotropic line width parameter was employed. To reproduce the widths of the isolated components, a correlated Gaussian distribution of *g*-values and *A*(Cu)-values were included as well. Reported Cu-hyperfine coupling constants are of the ^{63}Cu isotope. $A(^{65}Cu)$ can be calculated using a conversion factor of 1.0711 (difference in the gyromagnetic ratios of the nuclei).

Since the separation between peaks in the superfine structure in the range between 328 and 335 G (best visible in the second derivative representation) is roughly equal to the ^{14}N HF coupling constants, the uncertainty in $A_{iso}(^{14}N)$ is estimated on the basis of the residual difference between the simulation and the experimental data in this range, as illustrated in Figure S1B in the Supporting Information.

RESULTS AND DISCUSSION

In the lowest energy structure found for the negatively charged Cu−PS_2 cluster, Cu^{2+} was bound to the amine and carboxylate on the headgroup of two PS lipids, with the nitrogen centers *cis* to each other and the oxygen centers also *cis* to each other. In this structure, Cu^{2+} was also bound to one water molecule, resulting in a square pyramidal geometry. As has been noted previously, Cu^{2+} likely binds to the two amino and two carboxylate groups because of its relatively high affinity for these moieties.[50] Additionally, a square pyramidal structure is not surprising, as a coordination number of 5 is common for Cu^{2+} complexes.[51] The *cis* and *trans* structures of the Cu−PS_2 cluster are shown in Figures 2a, 2b. According to these calculations, the *cis* conformer will be extremely more abundant at physiological temperatures (e.g., 37 °C), as it is lower in

DOI: 10.1021/acs.jpcb.6b10675
J. Phys. Chem. B 2016, 120, 12883−12889

energy than the *trans* conformer by 6.5−8.3 kcal/mol (Table 1), which corresponds to an equilibrium constant on the order of 10^4−10^6.

Table 1. Relative Energies of the *cis* and *trans* Conformations of Cu(II)−Bis(glycinato) Monohydrate and the Cu−PS_2 Cluster Model, Where ΔG Is the Free Energy of the *trans* Conformation Minus the Free Energy of the *cis* Conformation in kcal/mol

functional	ΔG (Cu−PS_2)	ΔG (Cu(II)−bis(glycinato))
B3LYP-D3	8.28	−1.38
M06	6.45	−2.30
M06-L	7.29	−2.76

The comparison of the neutral and negatively charged cluster energetics revealed that it was more favorable for the Cu−PS_2 system to be negatively charged than to be electrically neutral (Table 2). The lowest-energy structure found for the neutral Cu−PS_2 cluster is shown in Figure 2c. The energetic preference for Cu^{2+} to be bound to the amine and carboxylate groups on two separate PS lipids is in agreement with experimental data.[16,17]

Table 2. Preference of Negatively Charged over Neutral Cu−PS_2 Systems, That Is, the Difference in Free Energy between the Left Side of eq 1 and the Right Side of eq 1

functional	strength of preference (kcal/mol)
B3LYP-D3	15.82
M06	13.32
M06-L	17.24

EPR spectroscopic investigations augmented with calculations of EPR parameters by DFT provide additional support for the DFT calculations that show the *cis* structure is the preferred conformation. The X-band CW EPR measurements of Cu^{2+} in 50 mol % POPS/50 mol % POPC vesicles showed a well-defined signal with a typical Cu^{2+} hyperfine splitting pattern (Figure 3). The high-field component of the spectrum exhibits a fine structure that is attributed to a hyperfine interaction with two strongly coupled ^{14}N nuclei. Vesicles prepared in D_2O showed an increased resolution of this fine structure.

Pezzato et al.[52] studied the temperature dependence of the conformation of the Cu(II)−bis(glycinato) complex, in which the ^{14}N HF coupling constants were found to be markedly different for *cis* and *trans* isomers: 33 and 29 MHz, respectively. Moreover, the ^{14}N HF coupling seems to be very consistent across different bis(amino acidato)copper(II) complexes.[21] As our EPR analysis of the samples results in a well-defined ^{14}N HF splitting that corresponds to an A_{iso} = 33 MHz coupling constant, we conclude that the experimentally observed EPR spectrum can be attributed to the *cis* isomer. Moreover, since all parameters for the *g*-matrix and the $^{63/65}Cu$ and ^{14}N hyperfine couplings are expected to be somewhat different for the *cis* and *trans* conformers, the fact that the spectrum can be fit well with only one set of parameters indicates that the *cis* isomer is dominant in the sample.

In order to confirm the experimental EPR results, parameters for the *cis* and *trans* conformers were computed using DFT and compared to the experimental parameters (Table 3). Although the calculated *cis* and *trans* *g*-matrices are quite similar, the ^{14}N hyperfine coupling constants show much closer agreement with

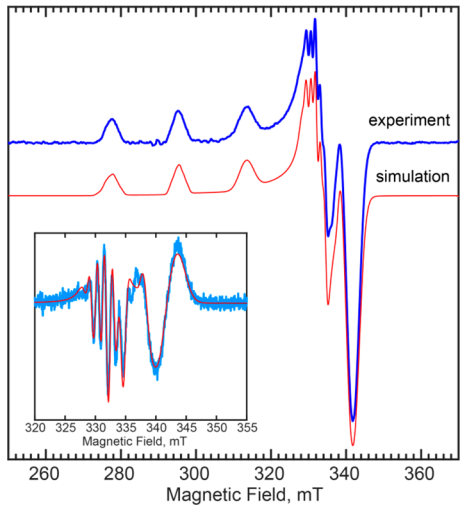

Figure 3. X-band CW EPR spectrum of Cu^{2+} with 50 mol % POPS/50 mol % POPC vesicles in 10 mM MOPS buffer containing 100 mM NaCl and 200 μM $CuCl_2$ in D_2O at pH 7.4 measured at 70 K (blue) and the corresponding simulation (red). The inset shows the derivative of the high-field part of the experimental spectrum (blue) and the simulation (red), emphasizing the ^{14}N fine structure. The simulation was obtained using the following spin-Hamiltonian parameters: g = [2.0550, 2.0583, 2.2582], $A(^{63}Cu)$ = [45, 45, 557] MHz, $A_{iso}(^{14}N)$ = 33 MHz, g_{Strain} = [0.013, 0.00, 0.00], g_{Dist}^{cor} = [0.00, 0.007, 0.014], $A_{Dist}^{cor}(^{63}Cu)$ = [0, −10, −60] MHz. The experimental conditions were as follows: temperature, 70 K; MW frequency, 9.625 GHz; MW power, 2 mW; modulation amplitude, 2 G; time constant, 40.96 ms, conversion time, 40 ms.

the *cis* structure than with the *trans* (Table 3). This is seen to a greater extent with B3LYP and M06 than with M06-L. However, this is to be expected, as it has previously been found that hybrid functionals are better suited for the prediction of EPR parameters.[53] The fact that the experimental EPR parameters are relatively close to those of the computationally determined *cis* structure, especially when using the hybrid functionals, supports the conclusion that the *cis* isomer is dominant.

To investigate the reason for the *cis* preference of the Cu−PS_2 system, energetics of smaller models containing only the immediate Cu^{2+} binding environment were compared. These Cu(II)−bis(glycinato) systems showed a small preference (Table 2) for the *trans* isomer compared to the *cis* isomer (Figure 4). The *trans* preference in the Cu(II)−bis(glycinato) system is in agreement with previous *ab initio* calculations[20,34,52,54] and may be due to lower electrostatic repulsion between the carboxylate groups in the *trans* isomer. Because this system shows an opposite conformational preference compared with the Cu−PS_2 model, the *cis* preference in the Cu−PS_2 model should be related to the presence of the phosphate, diacylglycerol and long carbon chains that make up the rest of the lipid. From an examination of the structures (Figure 5), the lower energy of the *cis* structure compared to the *trans* structure can be attributed to the extra stabilization of hydrogen bonds between the amino and phosphate groups as well as the more favorable electrostatic interactions between the parallel alkyl lipid chains, which are closer together in the *cis* conformer.

Now that the stereochemistry for the binding of Cu^{2+} to PS lipids has been revealed, it is reasonable to begin investigating the physiological consequences of this geometry. It has recently

DOI: 10.1021/acs.jpcb.6b10675
J. Phys. Chem. B 2016, 120, 12883−12889

Table 3. Computed and Experimental EPR Parameters, with Hyperfine Coupling Constants for Two Nonequivalent Nitrogen Atoms (N_A and N_B) Shown in MHz

functional	conformation	$A_{iso}(^{14}N_A)$	$A_{iso}(^{14}N_B)$	g_{xx}	g_{yy}	g_{zz}
B3LYP	*cis*	33.92	32.78	2.04	2.05	2.16
	trans	29.42	29.34	2.05	2.05	2.17
M06	*cis*	34.36	33.13	2.05	2.07	2.29
	trans	29.75	29.66	2.06	2.07	2.31
M06-L	*cis*	36.67	35.35	2.03	2.04	2.11
	trans	32.14	31.95	2.03	2.04	2.11
experiment		33 (±1)	33 (±1)	2.06	2.06	2.26

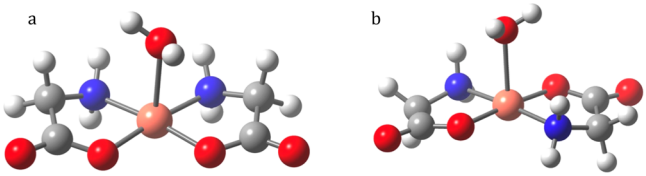

Figure 4. Optimized structures of the *cis* (a) and *trans* (b) configurations of Cu(II)−bis(glycinato) monohydrate (carbon is gray, copper is salmon, hydrogen is white, nitrogen is blue, and oxygen is red).

been shown that Cu^{2+} bound to lipids containing free amines (like phosphatidylethanolamine but also PS) can lead to lipid oxidation.[15] The geometry of binding may control the rate of oxidation as binding sites deeper into the membrane headgroup region may aid in the oxidation of double bonds deeper within the membrane structure. Next, it has been found that lipid domain formation is not induced by $Cu-PS_2$ complex formation. It was previously postulated that this result may be a consequence of the negative charge on each complex, which should cause repulsion between complexes. Since it is now known that these complexes are in the *cis* conformation, it can be further stated that they should lie relatively flat within the membrane and resist curvature effects that can also lead to domain formation. Finally, unlike cations such as Ca^{2+} or Zn^{2+}, the addition of Cu^{2+} to PS-containing vesicles does not promote vesicle fusion at μM Cu^{2+} concentrations or lower. Like with domain formation, the tendency for bivalent complexes to lie within the membrane plane probably influences this. If, instead, *trans* complexes had been formed, it might have been easier to link vesicles together or cause membrane fusion. The next step going forward will be to understand how transition metal ions like Cu^{2+} from the Irving−Williams series influence the physical properties of metallomembranes. Just like with the structure formed by transition metal ions binding to proteins to form metalloproteins, the structure of metallomembranes might also be linked to function and physical properties. This prospect should now be explored.

CONCLUSIONS

For the first time, we have identified the stereochemistry of an ion bound to two lipid headgroups. Results from the computed energy differences, EPR experiments, and EPR calculations definitively show that the Cu^{2+}−PS complex adopts a *cis* conformation. This is remarkable considering that the bis(glycinato)copper(II) complex, which has an identical primary coordination sphere as the $Cu^{2+}-PS_2$ complex, prefers the *trans* conformation. The *cis* preference of the Cu^{2+}−PS complex may be caused by more favorable hydrogen bonding between the amino and phosphate groups and electrostatic interactions between the lipid chains. These results suggest that, when Cu^{2+} is bound to PS lipids *in vitro*, it should form a *cis* complex. This is significant because it predicts that, other than linking two adjacent lipids together,[17] Cu^{2+} can bind to PS lipids without significantly perturbing the order of lipids within the bilayer.

ASSOCIATED CONTENT

Supporting Information

The Supporting Information is available free of charge on the ACS Publications website at DOI: 10.1021/acs.jpcb.6b10675.

Computational details, primarily Cartesian coordinates with their associated energies (PDF)

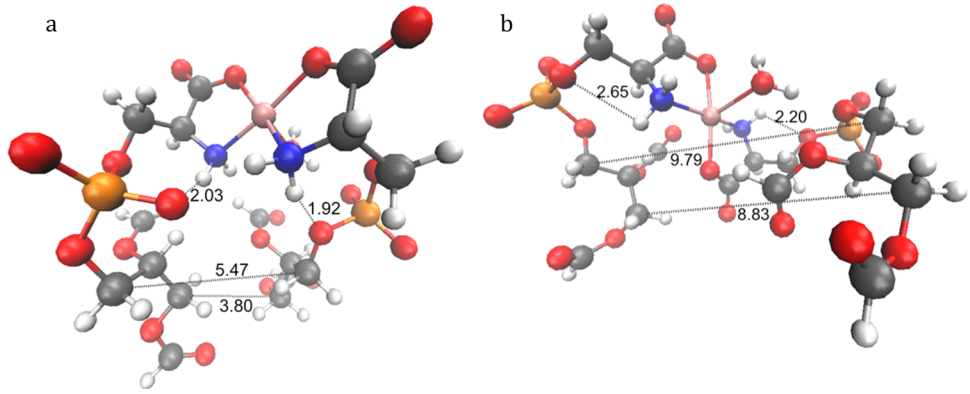

Figure 5. Optimized structures of the *cis* (a) and *trans* (b) configurations of PS bound to Cu^{2+}, showing the smallest distances (in Å) between the amino hydrogens and phosphate oxygens, as well as selected carbon atoms in the carbon backbone (carbon is gray, copper is salmon, hydrogen is white, nitrogen is blue, oxygen is red, and phosphorus is orange). Images were created with VMD.[49]

DOI: 10.1021/acs.jpcb.6b10675
J. Phys. Chem. B 2016, 120, 12883−12889

AUTHOR INFORMATION

Corresponding Authors

*E-mail: psc11@psu.edu.
*E-mail: gagliard@umn.edu.

ORCID

Paul S. Cremer: 0000-0002-8524-0438
Laura Gagliardi: 0000-0001-5227-1396

Present Address

§S.O.O.: Chemistry Department, University of Nevada Reno, 1664 N. Virginia Street, Reno, NV 89557.

Author Contributions

The manuscript was written through contributions of all authors. All authors have given approval to the final version of the manuscript.

Notes

The authors declare no competing financial interest.

ACKNOWLEDGMENTS

The computational and theoretical part of this work was supported in part by the U.S. Department of Energy, Office of Basic Energy 1090 Sciences, under SciDAC Grant No. DE-SC0008666. The experimental lipid chemistry was supported by grants from the National Science Foundation (CHE-1413307) and the Office of Naval Research (N00014-14-1-0792) to P.S.C. The Minnesota Supercomputing Institute provided part of the computational resources for this work.

REFERENCES

(1) Leventis, P. A.; Grinstein, S. The Distribution and Function of Phosphatidylserine in Cellular Membranes. *Annu. Rev. Biophys.* **2010**, *39* (1), 407−427.

(2) Schlegel, R. A.; Williamson, P. Phosphatidylserine, a Death Knell. *Cell Death Differ.* **2001**, *8*, 551−563.

(3) Lentz, B. R. Exposure of Platelet Membrane Phosphatidylserine Regulates Blood Coagulation. *Prog. Lipid Res.* **2003**, *42* (5), 423−438.

(4) Richter, R. P.; Lai Kee Him, J.; Tessier, B.; Tessier, C.; Brisson, A. R. On the Kinetics of Adsorption and Two-Dimensional Self-Assembly of Annexin A5 on Supported Lipid Bilayers. *Biophys. J.* **2005**, *89* (5), 3372−3385.

(5) Brose, N.; Petrenko, A. G.; Sudhof, T. C.; Jahn, R. Synaptotagmin: A Calcium Sensor on the Synaptic Vesicle Surface. *Science (Washington, DC, U. S.)* **1992**, *256* (5059), 1021−1025.

(6) Yeung, T.; Gilbert, G. E.; Shi, J.; Silvius, J.; Kapus, A.; Grinstein, S. Membrane Phosphatidylserine Regulates Surface Charge and Protein Localization. *Science (Washington, DC, U. S.)* **2008**, *319* (5860), 210−213.

(7) McLaughlin, S.; Mulrine, N.; Gresalfi, T.; Vaio, G.; McLaughlin, A. Adsorption of Divalent-Cations to Bilayer Membranes Containing Phosphatidylserine. *J. Gen. Physiol.* **1981**, *77* (4), 445−473.

(8) Ross, M.; Steinem, C.; Galla, H.-J.; Janshoff, A. Visualization of Chemical and Physical Properties of Calcium-Induced Domains in DPPC/DPPS Langmuir−Blodgett Layers. *Langmuir* **2001**, *17* (8), 2437−2445.

(9) Boettcher, J. M.; Davis-Harrison, R. L.; Clay, M. C.; Nieuwkoop, A. J.; Ohkubo, Y. Z.; Tajkhorshid, E.; Morrissey, J. H.; Rienstra, C. M. Atomic View of Calcium-Induced Clustering of Phosphatidylserine in Mixed Lipid Bilayers. *Biochemistry* **2011**, *50* (12), 2264−2273.

(10) Hinderliter, A. K.; Huang, J.; Feigenson, G. W. Detection of Phase Separation in Fluid Phosphatidylserine/phosphatidylcholine Mixtures. *Biophys. J.* **1994**, *67* (5), 1906−1911.

(11) Jacobson, K.; Papahadjopoulos, D. Phase Transitions and Phase Separations in Phospholipid Membranes Induced by Changes in Temperature, pH, and Concentration of Bivalent Cations. *Biochemistry* **1975**, *14* (1), 152−161.

(12) Silvius, J. R.; Gagne, J. Lipid Phase Behavior and Calcium-Induced Fusion of Phosphatidylethanolamine-Phosphatidylserine Vesicles. Calorimetric and Fusion Studies. *Biochemistry* **1984**, *23* (14), 3232−3240.

(13) Schultz, Z. D.; Pazos, I. M.; McNeil-Watson, F. K.; Lewis, E. N.; Levin, I. W. Magnesium Induced Lipid Bilayer Microdomain Reorganizations: Implications for Membrane Fusion. *J. Phys. Chem. B* **2009**, *113* (29), 9932−9941.

(14) Martín-Molina, A.; Rodríguez-Beas, C.; Faraudo, J. Effect of Calcium and Magnesium on Phosphatidylserine Membranes: Experiments and All-Atomic Simulations. *Biophys. J.* **2012**, *102* (9), 2095−2103.

(15) Poyton, M. F.; Sendecki, A. M.; Cong, X.; Cremer, P. S. Cu^{2+} Binds to Phosphatidylethanolamine and Increases Oxidation in Lipid Membranes. *J. Am. Chem. Soc.* **2016**, *138* (5), 1584−1590.

(16) Monson, C. F.; Cong, X.; Robison, A. D.; Pace, H. P.; Liu, C.; Poyton, M. F.; Cremer, P. S. Phosphatidylserine Reversibly Binds Cu^{2+} with Extremely High Affinity. *J. Am. Chem. Soc.* **2012**, *134* (18), 7773−7779.

(17) Cong, X.; Poyton, M. F.; Baxter, A. J.; Pullanchery, S.; Cremer, P. S. Unquenchable Surface Potential Dramatically Enhances Cu^{2+} Binding to Phosphatidylserine Lipids. *J. Am. Chem. Soc.* **2015**, *137* (24), 7785−7792.

(18) D'Angelo, P.; Bottari, E.; Festa, M. R.; Nolting, H.-F.; Pavel, N. V. X-Ray Absorption Study of Copper(II)−Glycinate Complexes in Aqueous Solution. *J. Phys. Chem. B* **1998**, *102* (17), 3114−3122.

(19) O'Brien, P. The Preparation and Characterization of the Geometric Isomers of a Coordination Complex: Cis- and Trans-Bis-Glycinato copper(II) Monohydrates. *J. Chem. Educ.* **1982**, *59* (12), 1052.

(20) Sabolović, J.; Tautermann, C. S.; Loerting, T.; Liedl, K. R. Modeling Anhydrous and Aqua Copper(II) Amino Acid Complexes: A New Molecular Mechanics Force Field Parametrization Based on Quantum Chemical Studies and Experimental Crystal Data. *Inorg. Chem.* **2003**, *42* (7), 2268−2279.

(21) Bukharov, M. S.; Shtyrlin, V. G.; Mukhtarov, A. S.; Mamin, G. V.; Stapf, S.; Mattea, C.; Krutikov, A. A.; Il'in, A. I.; Serov, N. Y. Study of Structural and Dynamic Characteristics of Copper(II) Amino Acid Complexes in Solutions by Combined EPR and NMR Relaxation Methods. *Phys. Chem. Chem. Phys.* **2014**, *16*, 9411−9421.

(22) Goodman, B. A.; McPhail, D. B.; Powell, H. K. Electron Spin Resonance Study of Copper(II)-Amino-Acid Complexes: Evidence for *Cis* and *Trans* Isomers and the Structures of Copper(II)-Histidine Complexes in Aqueous Solution. *J. Chem. Soc., Dalton Trans.* **1981**, No. 3, 822−827.

(23) Gutten, O.; Beššeová, I.; Rulíšek, L. Interaction of Metal Ions with Biomolecular Ligands: How Accurate Are Calculated Free Energies Associated with Metal Ion Complexation? *J. Phys. Chem. A* **2011**, *115* (41), 11394−11402.

(24) Tissandier, M. D.; Cowen, K. A.; Feng, W. Y.; Gundlach, E.; Cohen, M. H.; Earhart, A. D.; Coe, J. V.; Tuttle, T. R., Jr. The Proton's Absolute Aqueous Enthalpy and Gibbs Free Energy of Solvation from Cluster-Ion Solvation Data. *J. Phys. Chem. A* **1998**, *102* (98), 7787−7794.

(25) Frisch, M. J.; Trucks, G. W.; Schlegel, H. B.; Scuseria, G. E.; Robb, M. A.; Cheeseman, J. R.; Scalmani, G.; Barone, V.; Mennucci, B.; Petersson, G. A.; et al. *Gaussian 09*; Gaussian, Inc.: Wallington, CT, 2009.

(26) Perdew, J. P.; Ernzerhof, M.; Burke, K. Rationale for Mixing Exact Exchange with Density Functional Approximations. *J. Chem. Phys.* **1996**, *105*, 9982−9985.

(27) Becke, A. D. Density-Functional Exchange-Energy Approximation with Correct Asymptotic Behavior. *Phys. Rev. A: At., Mol., Opt. Phys.* **1988**, *38* (6), 3098−3100.

(28) Becke, A. D. Density-Functional thermochemistry.III. The Role of Exact Exchange. *J. Chem. Phys.* **1993**, *98* (7), 5648−5652.

(29) Grimme, S.; Antony, J.; Ehrlich, S.; Krieg, H. A Consistent and Accurate *Ab Initio* Parametrization of Density Functional Dispersion

DOI: 10.1021/acs.jpcb.6b10675
J. Phys. Chem. B 2016, 120, 12883−12889

Correction (DFT-D) for the 94 Elements H-Pu. *J. Chem. Phys.* **2010**, *132* (15), 154104−154119.
(30) Zhao, Y.; Truhlar, D. G. A New Local Density Functional for Main-Group Thermochemistry, Transition Metal Bonding, Thermochemical Kinetics, and Noncovalent Interactions. *J. Chem. Phys.* **2006**, *125* (19), 194101−194118.
(31) Zhao, Y.; Truhlar, D. G. The M06 Suite of Density Functionals for Main Group Thermochemistry, Thermochemical Kinetics, Noncovalent Interactions, Excited States, and Transition Elements: Two New Functionals and Systematic Testing of Four M06-Class Functionals and 12 Other Function. *Theor. Chem. Acc.* **2008**, *120* (1), 215−241.
(32) Weigend, F.; Ahlrichs, R. Balanced Basis Sets of Split Valence, Triple Zeta Valence and Quadruple Zeta Valence Quality for H to Rn: Design and Assessment of Accuracy. *Phys. Chem. Chem. Phys.* **2005**, *7* (18), 3297.
(33) Weigend, F. Accurate Coulomb-Fitting Basis Sets for H to Rn. *Phys. Chem. Chem. Phys.* **2006**, *8* (9), 1057.
(34) de Bruin, T. J. M.; Marcelis, A. T. M.; Zuilhof, H.; Sudhölter, E. J. R. Geometry and Electronic Structure of Bis-(Glycinato)-Cu^{II}·$2H_2O$ Complexes as Studied by Density Functional B3LYP Computations. *Phys. Chem. Chem. Phys.* **1999**, *1* (18), 4157−4163.
(35) Bryantsev, V. S.; Diallo, M. S.; Goddard, W. A. Computational Study of Copper(II) Complexation and Hydrolysis in Aqueous Solutions Using Mixed Cluster/Continuum Models. *J. Phys. Chem. A* **2009**, *113* (34), 9559−9567.
(36) Rulíšek, L.; Havlas, Z. Theoretical Studies of Metal Ion Selectivity. 1. DFT Calculations of Interaction Energies of Amino Acid Side Chains with Selected Transition Metal Ions (Co^{2+}, Ni^{2+}, Cu^{2+}, Zn^{2+}, Cd^{2+}, and Hg^{2+}). *J. Am. Chem. Soc.* **2000**, *122* (42), 10428−10439.
(37) Remko, M.; Rode, B. M. Effect of Metal Ions (Li^+, Na^+, K^+, Mg^{2+}, Ca^{2+}, Ni^{2+}, Cu^{2+}, and Zn^{2+}) and Water Coordination on the Structure of Glycine and Zwitterionic Glycine. *J. Phys. Chem. A* **2006**, *110*, 1960−1967.
(38) Rulíšek, L.; Havlas, Z. Theoretical Studies of Metal Ion Selectivity. 2. DFT Calculations of Complexation Energies of Selected Transition Metal Ions (Co^{2+}, Ni^{2+}, Cu^{2+}, Zn^{2+}, Cd^{2+}, and Hg^{2+}) in Metal-Binding Sites of Metalloproteins. *J. Phys. Chem. A* **2002**, *106*, 3855−3866.
(39) E. P Serjeant, B. D. *Ionisation Constants of Organic Acids in Aqueous Solution; IUPAC No. 23*, 1st ed.; Pergamon Press: New York, 1979.
(40) Scalmani, G.; Frisch, M. J. Continuous Surface Charge Polarizable Continuum Models of Solvation. I. General Formalism. *J. Chem. Phys.* **2010**, *132* (11), 114110.
(41) te Velde, G.; Bickelhaupt, F. M.; Baerends, E. J.; Fonseca Guerra, C.; van Gisbergen, S. J. A.; Snijders, J. G.; Ziegler, T.; Velde, G. T. E.; Guerra, C. F.; van Gisbergen, S. J. A. Chemistry with ADF. *J. Comput. Chem.* **2001**, *22* (9), 931−967.
(42) Van Lenthe, E.; Baerends, E. J.; Snijders, J. G. Relativistic Regular Two-Component Hamiltonians. *J. Chem. Phys.* **1993**, *99* (6), 4597.
(43) van Lenthe, E.; Baerends, E. J.; Snijders, J. G. Relativistic Total Energy Using Regular Approximations. *J. Chem. Phys.* **1994**, *101* (11), 9783.
(44) Klamt, A.; Schüürmann, G. COSMO: A New Approach to Dielectric Screening in Solvents with Explicit Expressions for the Screening Energy and Its Gradient. *J. Chem. Soc., Perkin Trans. 2* **1993**, No. 5, 799−805.
(45) Pye, C. C.; Ziegler, T. An Implementation of the Conductor-like Screening Model of Solvation within the Amsterdam Density Functional Package. *Theor. Chem. Acc.* **1999**, *101*, 396−408.
(46) Hope, M. J.; Bally, M. B.; Webb, G.; Cullis, P. R. Production of Large Unilamellar Vesicles by a Rapid Extrusion Procedure. Charaterization of Size Distribution, Trapped Volume and Ability to Maintain a Membrane Potential. *Biochim. Biophys. Acta, Biomembr.* **1985**, *812*, 55.
(47) Mayer, L. D.; Hope, M. J.; Cullis, P. R. Vesicles of Variable Sizes Produced by a Rapid Extrusion Procedure. *Biochim. Biophys. Acta, Biomembr.* **1986**, *858*, 161.
(48) Silakov, A.; Epel, B. Kazan Viewer, https://sites.google.com/site/silakovalexey/kazan-viewer.
(49) Stoll, S.; Schweiger, A. EasySpin, a Comprehensive Software Package for Spectral Simulation and Analysis in EPR. *J. Magn. Reson.* **2006**, *178* (1), 42−55.
(50) Shirane, K.; Kuriyama, S.; Tokimoto, T. Synergetic Effects of Ca^{2+} and Cu^{2+} on Phase Transition in Phosphatidylserine Membranes. *Biochim. Biophys. Acta, Biomembr.* **1984**, *769* (3), 596−600.
(51) Rulíšek, L.; Vondrášek, J. Coordination Geometries of Selected Transition Metal Ions (Co^{2+}, Ni^{2+}, Cu^{2+}, Zn^{2+}, Cd^{2+}, and Hg^{2+}) in Metalloproteins. *J. Inorg. Biochem.* **1998**, *71* (3−4), 115−127.
(52) Pezzato, M.; Della Lunga, G.; Barratto, M. C.; Sinicropi, A.; Pogni, R.; Basosi, R. The *Cis*/*Trans* Isomerization of Cu(II)-Bis-(Glycinato) Complex in Solution: A Computer Aided Multifrequency EPR and DFT/PCM Calculation Study. *Magn. Reson. Chem.* **2007**, *45*, 846−849.
(53) Arbuznikov, A. V.; Kaupp, M.; Malkin, V. G.; Reviakine, R.; Malkina, O. L. Validation Study of Meta-GGA Functionals and of a Model Exchange-Correlation Potential in Density Functional Calculations of EPR Parameters. *Phys. Chem. Chem. Phys.* **2002**, *4* (22), 5467−5474.
(54) Lutz, O.; Messner, C.; Hofer, T. S.; Glätzle, M.; Huck, C. W.; Bonn, G. K.; Rode, B. M. Combined Ab Initio Computational and Infrared Spectroscopic Study of the *Cis*- and *Trans*-Bis (Glycinato) Copper (II) Complexes in Aqueous Environment. *J. Phys. Chem. Lett.* **2013**, *4* (Ii), 1502−1506.

DOI: 10.1021/acs.jpcb.6b10675
J. Phys. Chem. B 2016, 120, 12883−12889